sustainability

MDPI

Article

Risk Assessment of Single-Gully Debris Flow Based on Dynamic Changes in Provenance in the Wenchuan Earthquake Zone: A Case Study of the Qipan Gully

Na Su [1,*], Linrong Xu [1,2], Bo Yang [3], Yongwei Li [1] and Fengyu Gu [1]

[1] School of Civil Engineering, Central South University, Changsha 410075, China
[2] National Engineering Laboratory for High-Speed Railway Construction, Central South University, Changsha 410075, China
[3] College of Civil Engineering, Henan University of Technology, Zhengzhou 450001, China
* Correspondence: 184801021@csu.edu.cn

Abstract: After the Wenchuan earthquake on 12 May 2008, a huge amount of loose deposits was generated on the mountain surface in the earthquake zone, and vegetation was severely damaged, providing a rich source of material for debris flow, greatly increasing the danger. For many years, researchers have mainly considered the recovery of slope vegetation in assessing the risk of debris flow post-earthquake. However, field investigations have found that large amounts of the dynamic reserve materials in the gully have an important impact on the risk. Thus, based on field survey data, this paper takes the Qipan gully in Wenchuan County as an object and uses multi-source and multi-scale monitoring methods (Landsat series, Quickbird, and Unmanned Air Vehicle) to analyze and statistically study the provenance of the slope and gully both pre- and post- the earthquake. By comprehensively using game theory combination weighting and the cloud model, a dynamic risk assessment model for debris flow was constructed to evaluate the risk of debris flow from 2005 to 2019. The results show that the slope provenance post-earthquake was 7.7 times that of pre-earthquake, and by 2019 the slope provenance had recovered to the pre-earthquake level. Based on the statistical estimation of the amount of debris flow outbreak and the dredging of the blocking dam recorded in relevant data, the dynamic provenance of debris flow had decreased by about 781.3 $\times$ 10^4 m^3 by 2019. Compared with considering slope provenance only, the assessment result of debris flow risk considering both slope and gully provenance is more realistic. The results are expected to provide reference and guidance for dynamic assessment of the risk of debris flow faced by increasing projects in high-seismic-intensity mountainous areas and to ensure the safety of people's lives and property effectively.

Keywords: Wenchuan earthquake; debris flow; changes in provenance; combination weighting method; cloud model; risk assessment

check for updates

Citation: Su, N.; Xu, L.; Yang, B.; Li, Y.; Gu, F. Risk Assessment of Single-Gully Debris Flow Based on Dynamic Changes in Provenance in the Wenchuan Earthquake Zone: A Case Study of the Qipan Gully. *Sustainability* **2023**, *15*, 12098. https://doi.org/10.3390/su151512098

Academic Editors: Yang Wu, Norimasa Yoshimoto and Rongtao Yan

Received: 11 April 2023
Revised: 24 July 2023
Accepted: 4 August 2023
Published: 7 August 2023

Copyright: © 2023 by the authors. Licensee MDPI, Basel, Switzerland. This article is an open access article distributed under the terms and conditions of the Creative Commons Attribution (CC BY) license (https://creativecommons.org/licenses/by/4.0/).

1. Introduction

On 12 May 2008, an earthquake with a magnitude of Richter (MS) 8.0 struck Wenchuan County in Sichuan Province, China, triggering over 56,000 landslides [1]. Under the influence of heavy rainfall, these landslides frequently transformed into debris flows, rapidly increasing the danger in the region and posing a great threat to the production and livelihoods of residents [2,3]. The most devastating debris flow disasters occurred in Longchi Town and Yingxiu Town on 14 August 2010, as well as in Wenchuan County on 10 July 2013, and 20 August 2019 [4]. At present, research about the duration of debris flow post-earthquake is a hotspot, and the overwhelming majority believe that it would last for approximately 20–30 years. Huang et al. [5] summarized the characteristics and occurrence rules of geological disasters for 3 years after the Wenchuan earthquake and found that group-occurring debris flow is the dominant type of geological disaster and estimated an active period of 20–25 years. Based on 8 years of investigation of the vegetation recovery

process post-earthquake, Yang et al. [6] estimated that it would take 20 years for vegetation to recover to the pre-earthquake level. Fan et al. [7] analyzed debris flow activities in Gaojiagou during 2008–2016. They verified the strong correlation between the evolution of deposits and the scale of debris flow and found a decrement of 60% in slope provenance in 2016. Chen et al. [8] studied a debris flow in 2019 and found that gully provenance is the dominating factor in the long-term persistence of debris flow. Most existing studies have yet to quantitatively analyze the dynamic variations in gully provenance, especially the artificially reduced volume of gully provenance after the construction of blocking structures, which would lead to deviations in the assessment of the scale and frequency of debris flows.

Provenance refers to the loose deposits induced by geological and human activities, and is the material source of debris flow. Slope provenance, induced by unfavorable geological bodies such as landslides, collapses, and debris flows, is the main portion of provenance and is located on gullies. Over time, a part flows into a gully with rainfall and supplies the gully provenance, and the rest are covered by vegetation. The gully provenance, influenced by terrain, landform, and catchment area, plays a dominant role in the occurrence of future debris flow [9]. Li et al. [4] surveyed the Chediguan gully debris flow that occurred on 20 August 2019, with Unmanned Air Vehicle (UAV) and high-definition remote sensing interpretation to analyze the formation mechanism and dynamic characteristics and found that this large-scale debris flow 11 years after the Wenchuan earthquake is induced by the runoff erosion of gully deposits derived from the deposition of slope provenance. This is different from the formation mechanism of the debris flow initiated by a landslide in 2010. Based on an interpretation of multi-source remote sensing images, Fan et al. [10] discovered that the total number of slope provenance decreased from 9189 in 2008 to 221 in 2015. In addition, new slope provenance could be found from new images post-earthquake, and the numbers were 781, 360, and 8 in 2011, 2013, and 2015, respectively. Hence, multiple approaches and methods for monitoring should be adopted to "gaze" the study area for a long time to acquire the dynamic evolution of slope provenance more precisely [11–14]. On the basis of this, the gully provenance could be determined and the risk assessment of debris flow would be more realistic.

Hazard evolution, duration, and the relationship with the provenance of debris flow are the focus of research. Various random, fuzzy, and uncertain factors are involved in the assessment of debris flow for its complexity and nonlinearity [15–17]. Since the 1970s, research about the risk assessment of debris flow has been carried out and various methods, such as qualitative analysis method, based on expert evaluation and fuzzy analytic hierarchy process, and quantitative evaluation of statistical analysis represented by machine learning, for instance grey relational analysis and the random forest and BP neural network approach, have been proposed. Nevertheless, the methods mentioned before are not suitable for debris flow in a single gully due to the strong subjective randomness of qualitative assessment and huge difficulties in collecting massive historical data for quantitative analysis. As a mathematical model that combines probability theory and fuzzy mathematics for the interconversion of qualitative and quantitative analysis, the cloud model could substitute the traditional function of the membership degree and effectively balance the existing randomness and fuzziness of the evaluation object, which greatly improves the credibility of the results [18–21]. Hence, it is necessary to employ game theory combination weighing and the cloud model to construct a model for the risk assessment of debris flow. For frequent debris flow in history and a main gully length of 15.2 km, plenty of gully provenance could be observed in the Qipan gully in Wenchuan County. In addition, the construction of five blocking dams in 2014 makes it a typical representative to evaluate the influence of variation in slope and gully provenance post-earthquake on the risk of debris flow. This study takes the Qipan gully as its objective to explore the influences of variation in the disaster-pregnant environment on the risk of debris flow during 2005–2019 and to predict development tendency. The ultimate aim of this study is to provide new insight into the promotion of modernization and conscientization of disaster prevention

and optimization of the deployment of disaster prevention and mitigation resources, which is of high scientific and technological value and strategic significance.

2. Study Area

The Qipan gully is located in Weizhou Town, about 7 km southwest of Wenchuan County [22,23]. This gully, with a catchment area of 54.2 km^2 and a main gully length of 15.2 km, is a first-grade tributary at the upper Minjiang River. The subtropical semiarid monsoon climate in this area is characterized by a terrain that is significantly influenced by a low but concentrated rainfall, frequent local rainstorms, and hail (>20 mm). According to data from the Weizhou meteorological station, recorded over a period of 23 years, the annual average precipitation in this area is 528.7 mm and the precipitation is concentrated in the rain season from May to September [24]. The maximum precipitation of the rainy season is 324 mm, accounting for 62.1% of the annual precipitation. This area, characterized by relatively frequent seismic activity, is in the Jiuding Mountain Cathaysian tectonic zone, including the Maowen fault belt and the Jiuding Mountain fault belt. Based on local existing records, earthquakes occur frequently in this area, including eight major earthquakes and many strong earthquakes above MS 5.0, such as the Diexi MS 7.3 earthquake on 25 August 1933, and the Wenchuan MS 8.0 earthquake on 12 May 2008. The seismic ground motion parameter zonation map of China reveals that this gully is in a high-intensity seismic region (VIII degrees), with a peak ground acceleration of 0.2 g and a characteristic period of seismic response spectrum of 0.35s [25]. A terrain of leaf-vein shape in this area is composed of a main gully and 15 branches, with geomorphic features of rugged high mountains and deeply incised valleys. The altitude of the gully mouth is 1310 m and the maximum altitude is 4350 m with a longitudinal gradient of the main gully of 192‰, and a glacial erosion landform could be found at elevations above 3000 m. According to classification statistics of ArcGIS from the Digital Elevation Model (DEM), the terrain in this gully is steep and the area of mountain gradient beyond 30° is 65.11% of the total (Figure 1).

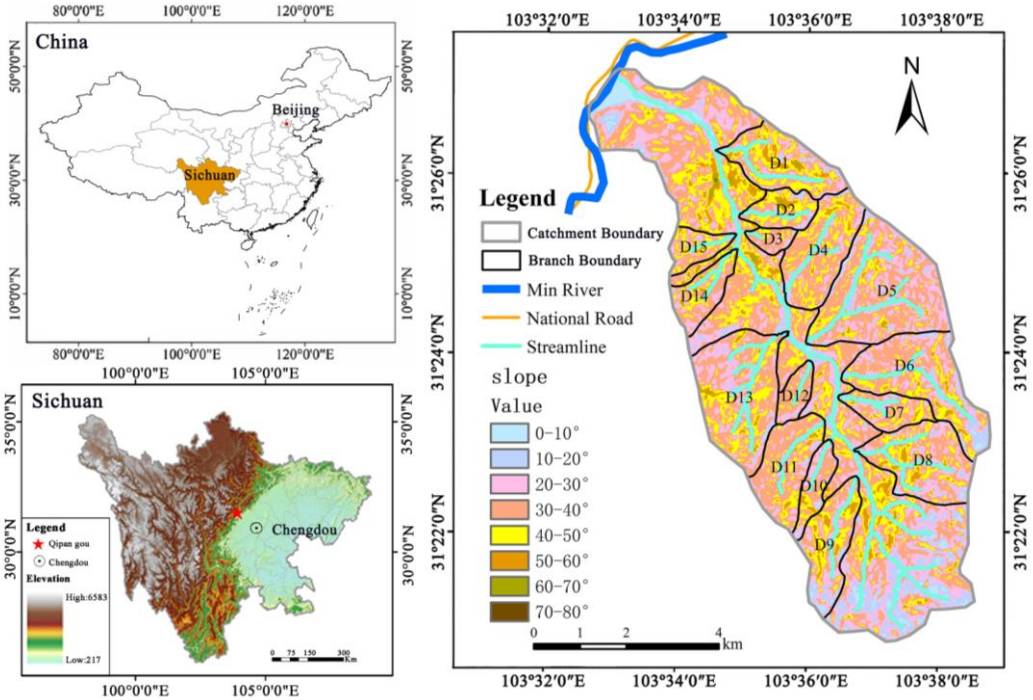

Figure 1. Location and terrain of the Qipan gully in Wenchuan County, Sichuan Province, China.

The branches of this gully are well developed and have water throughout the year mainly supplied by atmospheric precipitation, which is the source of local drinking water. The abundant loose deposits in this area are induced by frequent earthquakes, and in

combination with concentrated rainfall and steep terrain they greatly increase the possibility of debris flow. According to the literature, debris flows occurred frequently in the Qipan gully before the Wenchuan earthquake [26,27] (Table 1). For the safety of the life and property of downstream people, a drainage canal (3200 × 15 × 3 m in dimension) was built in 1980 but destroyed in the Wenchuan earthquake. Thereafter, a total volume of 26.2 million m^3 loose provenance was produced according to the field investigation and many debris flow events occurred in the gully, according to field investigation reports. Especially on 11 July 2013, under the influence of a 24 h rainfall of 54.3 mm, a large-scale debris flow occurred and the single outburst volume was 78.2 × 10^4 m^3 [28].

Table 1. Historical debris flow events that have occurred in the Qipan catchment [27].

Time	Daily Precipitation (mm)	Debris Flow Volume (10^4 m^3)	Damage	General Situations of the Projects
1933	Missing data	Missing data	Destroyed 1 village (Xuehuatan).	/
6 July 1961	79.9	13.5	Destroyed 1 bridge, roadbed of 0.4 km; traffic interruption of 15 days.	/
23 July 1964	41.7	9.1	Destroyed 3 bridges, roadbed of 4 km; buried farmland of 4.0 hectares.	/
28 July 1970	33.0	5.8	Destroyed 4 bridges, roadbed of 5 km; buried farmland of 5.3 hectares.	/
24 July 1971	53.4	8.4	Destroyed 5 bridges, roadbed of 8 km; buried farmland of 8.0 hectares.	/
29 July 1975	32.5	9.8	Destroyed a roadbed of 4 km; buried farmland of 2.7 hectares.	/
7 July 1977	39.4	5.8	Destroyed 5 bridges, a roadbed of 4 km, and 1 drainage channel.	/
15 July 1978	66.7	13.5	Destroyed 4 km of forest road, 5 bridges, and the entire old drainage channel, endangered factory safety with a direct economic loss of 49,000 yuan.	/
15 August 1979	30.8	3.8	No damage.	/
26 July 1980	Missing data	5.4	No damage.	Drainage channel with a length of 3200 m
12 August 1981	53.8	6.7	No damage.	/
19 July 1983	31.3	2.3	No damage.	/
12 May 2008	Missing data	Missing data	Missing data	Forementioned drainage channel damaged
11 July 2013	54.3	78.2	8 people died, 6 people went missing, and 90% of the houses of residents in the area downstream were completely devastated.	Forementioned projects destroyed
2014-6	/	/	/	5 blocking dams and compound drainage channel
5 July 2017	18.6	18.5	No damage.	/
22 August 2018	33.4	11.5	No damage.	/
20 August 2019	28.1	15	No damage.	/

3. Methods

3.1. Source of Multi-Scale Data of Debris Flow

Based on the geological survey report and pertinent literature [29–31], a field investigation, UAV exploration, and multi-type and multi-temporal remote sensing were conducted to obtain a dynamic variation in provenance in the Qipan gully after the Wenchuan earthquake. The fundamental condition of this gully and single outburst volume was obtained by two field investigations: in October 2008, carried out by Sichuan Huadi Building Engineering Co., Ltd. (Chengdu, China). [29], and October 2013, conducted by Sichuan Shutong Geotechnical Engineering Company, respectively [30]. With the continuous development of remote sensing technology, more and more methods and approaches for acquiring data could be used. However, each method has its limitations [31]. Landsat series remote sensing images contain near-infrared bands, which could be classified by texture, spectrum, and other information. Vegetation information could be extracted with an object-based classification method, and the extraction results could be imported into ArcGIS to obtain vegetation coverage images [32]. This method is convenient and effective with a relatively low resolution. The Quickbird optical remote sensing has a high resolution of up to 0.5 m, which allows for clear observation of mountain vegetation. Thus, it is usually used to assist in the interpretation of dynamic variations in provenance. However, this method is seriously affected by weather conditions and in consideration of the highly variable weather in the study area it is relatively difficult to acquire suitable images [4]. In this study, the two aforementioned methods are employed and multiple sets of data including pre-earthquake, post-earthquake, and post-debris flow are selected to analyze vegetation recovery and to explore the evolution characteristics of slope provenance in the Qipan gully. The selected data are composed of Landsat 5 images (September 2005 and July 2008), Landsat 8 images (October 2013, June 2014, April 2017, and June 2019), and Quickbird data in September 2005, May 2008, April 2011, December 2014, April 2018 and October 2019. In addition, gully provenance is determined by the field investigation and UAV data carried out on 16 March 2019, and relevant literature and precipitation data are acquired from related meteorological records. To protect the safety of people's lives and property in the alluvial fan and roads in the gully mouth, a series of blocking projects designed according to a 50 years recurrence interval were built in this gully. The projects, including three check dams, two pile-group dams, and 1 silt dam, were completed in 2014 and are also an important reference for dynamic variations in gully provenance.

3.2. Risk Assessment of Debris Flow

Risk assessment is used to quantitatively characterize the probability of intensity scale of the disaster body and the frequency of debris flow in a time in the future, which is of a nonlinear and nondeterministic relationship to disaster-pregnant environmental elements [15]. The combination weighing method of game theory is capable of comprehensively considering the influence of subjective and objective information on assessment results and has obvious advantages in comparison with the traditional weighing method [16]. After combing it with the cloud model, the interconversion of qualitative and quantitative analysis could be implemented by the fusion of random functions of traditional probability theory and modern fuzzy mathematics [17]. Based on this, a hazard assessment model of debris flow is established in this study to reflect fuzziness and randomness during assessment by expectation (*Ex*), entropy (*En*), and hyper entropy (*He*).

3.2.1. Entropy Method

The entropy method could be employed to determine the objective weight and assess the risk of debris flow [33]. The specific steps are as follows:

a. Establishment matrix (R′) of original data (Equation (1)):

$$R' = \left(x_{ij}\right)_{n\times m} (i = 1, 2, \ldots, n,\ \ j = 1, 2, \ldots, m) \quad (1)$$

where x_i is the value of the j_{th} disaster-pregnant environment factor of the i_{th} sample, n is the number of samples and values as 6 in this study, and m is the number of factors and values as 14 in this study.

b. Standardization of x_{ij}, including the "larger-is-risker" type (Equation (2)) and the "smaller-is-risker" type (Equation (3)). The influence of various factors on the risk of debris flow needs to be standardized because the larger the value of some factors, the riskier it is and the rest are opposite. For instance, the smaller the vegetation coverage, the more prone it is to debris flow, which belongs to the "smaller-is-risker". The equations are listed below:

$$\gamma_{ij} = \frac{x_{ij} - \min(j)}{\max(j) - \min(j)} \tag{2}$$

$$\gamma_{ij} = \frac{\max(j) - x_{ij}}{\max(j) - \min(j)} \tag{3}$$

where γ_{ij} is the standardized value of x_{ij}, and max(j) and min(j) are the maximum value and minimum value of a factor, respectively.

c. Calculation of entropy (Equations (4) and (5)):

$$P_{ij} = \frac{\gamma_{ij}}{\sum_{j-1}^{n} \gamma_{ij}} \tag{4}$$

$$E_j = \frac{1}{\ln m} \sum_{i}^{m} P_{ij} \ln P_{ij} \tag{5}$$

where P_{ij} is the frequency of the i-th index in the debris flow, and E_j is the entropy of the j_{th} factor. When $\gamma_{ij} = 0$, $P_{ij} \ln P_{ij} = 0$.

d. Weight calculation (Equation (6)):

$$W(j) = \frac{1 - E_j}{\sum_{i=1}^{\mathrm{n}} (1 - \mathrm{E_j})} \tag{6}$$

where $W(j)$ is the weight of the j_{th} factor.

e. Risk value calculation (Equation (7)):

$$H(i) = \sum_{j=1}^{\mathrm{n}} W_{\mathrm{z}}(j) \gamma_{\mathrm{ij}} \tag{7}$$

where $H(i)$ is the risk value of debris flow in the i_{th} year.

3.2.2. Grey Relational Analysis Method (G1)

The G1 method is a multi-factor sorting method based on the theory of the grey system. In the G1 method, sovereignty and weight assignment refer to the determination of the weight of each factor in the ranking, also known as the main weight [34]. The principle of the G1 method is an inheritance of the idea of relative importance judgment of indicators from the analytic hierarchy process. The main steps are as follows:

a. Invite experts to rank the importance of assessment indicators for debris flow. Assuming the set of assessment indicators, M is:

$$M = (C_1, C_2, C_3, \cdots C_{j-1}, C_j, \cdots C_q) \tag{8}$$

where C_j is the $\mathrm{j_{th}}$ indicator, and q is the number of indicators. In this study, 14 indicators are considered; thus, q is 14.

b. Arrange all indicators in the set in a sequence of decreasing importance as follows:

$$C_1^* > C_2^* > \cdots > C_{j-1}^* > C_j^* > \cdots > C_q^* \tag{9}$$

c. Assign importance value by experts (in a sequence of decreasing importance) to all adjacent indicators (Equation (10)).

$$r_j = \frac{m_{j-1}}{m_j} \quad j = 2,\ 3,\ \cdots q \tag{10}$$

where r_j is the importance level between the $j-1$-th indicator and the j_{th} indicator. m_j is the weight of the j_{th} indicator.

d. According to the experts' assignment, calculate the subjective weight of the j_{th} indicator C_j*, and based on the ranking calculate the weights of all indicators. The calculation method is shown in Equation (11):

$$\begin{cases} w_j^* = \left(1 + \sum\limits_{i=2}^{j} \prod\limits_{k=i}^{j} r_k\right)^{-1} \\ w_{j-1}^* = r_j w_j^* \end{cases} \tag{11}$$

where w_j* is the weight of the j_{th} indicator. i = j, j − 1, j − 2, …, 3, 2.

3.2.3. Game Theory Combination Weighing

The determination of index weights is the basis of self-assessment. The combination weighting method could balance the advantages and disadvantages of subjective and objective weighing methods, taking into account both the actual laws of objective data and the decision-making intentions of evaluators. Game theory is an operational research method for studying competitive things, which could find the most balanced combination weight among index weights from various methods and make the index weighing more reasonable [35]. Based on the entropy method and G1 method, game theory is introduced into this study to determine the optimal combination weight with the following steps:

a. Denote the index weight obtained through entropy method and G1 method as w_1= (w_{11}, w_{12}, …, w_{1n}) and w_2= (w_{21}, w_{22}, …, w_{2n}), respectively. According to their linear combination, calculate combination weights with Equation (12):

$$w = \alpha_1 w_1^T + \alpha_2 w_2^T \tag{12}$$

where α_1 and α_2 are combination coefficients of subjective weight and objective weight, respectively.

b. Based on game theory, the Nash equilibrium point is obtained by seeking the balance between various weights, minimizing the deviation between the combination weight and the subjective and objective weights. The objective function and constraints are as follows in Equation (13):

$$\begin{aligned} \min(\|w - w_1^T\|_2 + \|w - w_2^T\|_2) = &\min(\|\alpha_1 w_1^T + \alpha_2 w_2^T - w_1^T\|_2 \\ &+ \|\alpha_1 w_1^T + \alpha_2 w_2^T - w_2^T\|_2) \end{aligned} \tag{13}$$

where $\alpha_1 + \alpha_2 = 1$ and $\alpha_1 \geq 0$, $\alpha_2 \geq 0$.

c. By solving this model, the optimal combination weight considering both subjective factors and objective data patterns can be obtained. This problem is to find the minimum value under equality constraints with the Lagrange function:

$$\begin{aligned} L(\alpha_1, \alpha_2, \lambda) = &\|\alpha_1 w_1^T + \alpha_2 w_2^T - w_1^T\|_2 + \|\alpha_1 w_1^T + \alpha_2 w_2^T - w_2^T\|_2 \\ &+ \tfrac{\lambda}{2}\left(\sum_{k=1}^{2} a_k - 1\right) \end{aligned} \tag{14}$$

where λ is the dangerousness coefficient.

d. According to the principle of differential calculus, the optimal first-order derivative condition of Equation (14) is as follows:

$$\begin{cases} \alpha_1 w_1 w_1^T + \alpha_2 w_1 w_2^T = w_1 w_1^T \\ \alpha_1 w_2 w_1^T + \alpha_2 w_2 w_2^T = w_2 w_2^T \end{cases} \tag{15}$$

e. The corresponding linear system of equations is as follows:

$$\begin{bmatrix} \begin{pmatrix} w_1 w_1^T \\ w_2 w_1^T \end{pmatrix} \begin{pmatrix} w_1 w_2^T \\ w_2 w_2^T \end{pmatrix} \end{bmatrix} \begin{bmatrix} \alpha_1 \\ \alpha_2 \end{bmatrix} = \begin{bmatrix} w_1 w_1^T \\ w_2 w_2^T \end{bmatrix} \tag{16}$$

f. According to Equation (16), α_1 and α_2 could be obtained and normalized:

$$a_i^* = \frac{|a_i|}{\sum_{i=1}^{2} a_i} \tag{17}$$

g. The optimal combination weight is as follows:

$$w^* = a_1^* w_1^T + a_2^* w_2^T \tag{18}$$

3.2.4. Establishment of the Cloud Model of Hazard Assessment of Debris Flow

The cloud model represents the random fuzziness of a concept both globally and locally through its numerical features; that is, expectation (E_x), entropy (E_n), and hyper entropy (H_e). Ex represents the standard value of a concept in the domain space, which is the point that best characterizes the concept qualitatively. E_n represents the range of a qualitative concept and measures the degree of uncertainty of the qualitative concept. He measures the degree of uncertainty of entropy and indirectly reflects the fuzziness of cloud droplets.

a. According to relevant literature [36], a bilateral constraint calculation formula is commonly employed to calculate cloud model parameters and is shown as follows (Equation (19)):

$$\begin{cases} E_x = \frac{(B_{max}+B_{min})}{2} \\ E_n = \frac{(B_{max}-B_{min})}{6} \\ H_e = k \end{cases} \tag{19}$$

where B_{max} and B_{min} are the maximum and minimum quantitative variables, respectively, and k is a constant.

b. He reflects the degree of uncertainty of E_n, which is a variable related to E_n, but the two are contradictory. Assume He is linear to E_n, and the relation could be expressed as follows (Equation (20)):

$$H_e = kE_n \tag{20}$$

k is 0.1 in this study to reflect the degree of discreteness of the qualitative index cloud map and make it more consistent with the actual assessment results.

c. A normal random variable $E_n{}'$ is generated with E_n as expectation and He as variance and denoted as follows (Equation (21)):

$$E_n' = NORM(E_n,\ H_e) \tag{21}$$

d. A normal random variable x is generated with E_x as expectation and $E_n{}'$ as variance and denoted as follows (Equation (22)):

$$x = NORM\left(E_x, E_n'\right) \tag{22}$$

e. Membership degree of the droplet could be calculated with Equation (23):

$$u = exp\left[\frac{(x - E_x)^2}{2(E_n')^2}\right] \tag{23}$$

f. The generated (x, u) is a droplet in the domain.

g. Repeat steps b–f until the desired n cloud droplets are generated.

A cloud model could be generated based on the above steps. The membership function of the normal cloud model could be generated by MATLAB. Any measured value of an indicator could be substituted into the function to obtain the membership degree d_{ij} in each level, where d_{ij} is the membership degree of the ith indicator in the corresponding jth level.

4. Variation in Debris Flow in the Qipan Gully

According to the literature [9,10,37] and field investigation, the provenance of post-earthquake debris flow varies dynamically, with an overall decrease trend. It is necessary to separately analyze the slope and gully provenance post-earthquake due to the huge difference in attenuation patterns between them. As shown in Figure 2, gully provenance flow out with the occurrence of debris flow or are blocked by the dams.

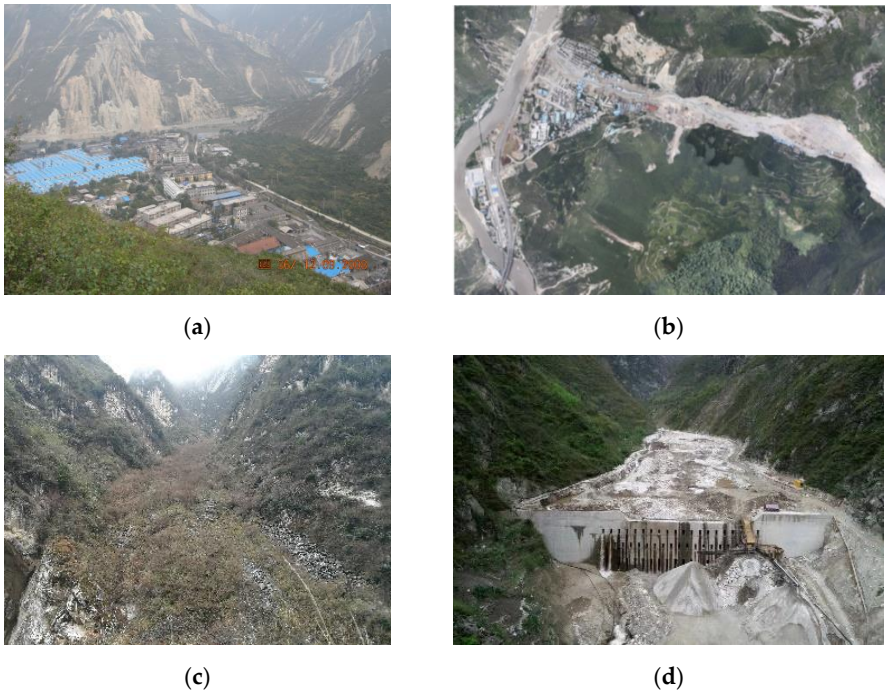

(**a**) (**b**) (**c**) (**d**)

Figure 2. Decrease patterns of provenance of debris flow in the Qipan gully. (**a**) Before the large-scale debris flow in 2013 (12 September 2008); (**b**) Occurrence of the large-scale debris flow (11 July 2013); (**c**) Vegetation fixes provenance (16 March 2019); (**d**) Dredging of blocking structures (16 March 2019).

4.1. Vegetation Coverage of the Qipan Gully during 2005–2019

The evolution of the slope provenance of debris flow post-earthquake mainly depends on dynamic changes in vegetation. The process of vegetation recovery could provide a basis for further understanding the influence duration of earthquake disasters. Six figures from 2005 to 2019 are obtained based on availability, coverage, cloud cover, and resolution, as shown in Figure 3. NDVI is considered as the most pivotal indicator in vegetation monitoring and could be calculated as follows [28]:

$$NDVI = \frac{NIR - R}{NIR + R} \tag{24}$$

where NIR is near-infrared band reflectance, and R is infrared band reflectance. The range of NDVI values is between −1 and 1. The higher the value, the better the vegetation coverage. NDVI could serve as an indicator of photosynthetic capacity, whose effectiveness in satellite assessment and vegetation dynamic monitoring has been well demonstrated. In this study, the vegetation recovery rate from NDVI is used to assess the process of vegetation recovery.

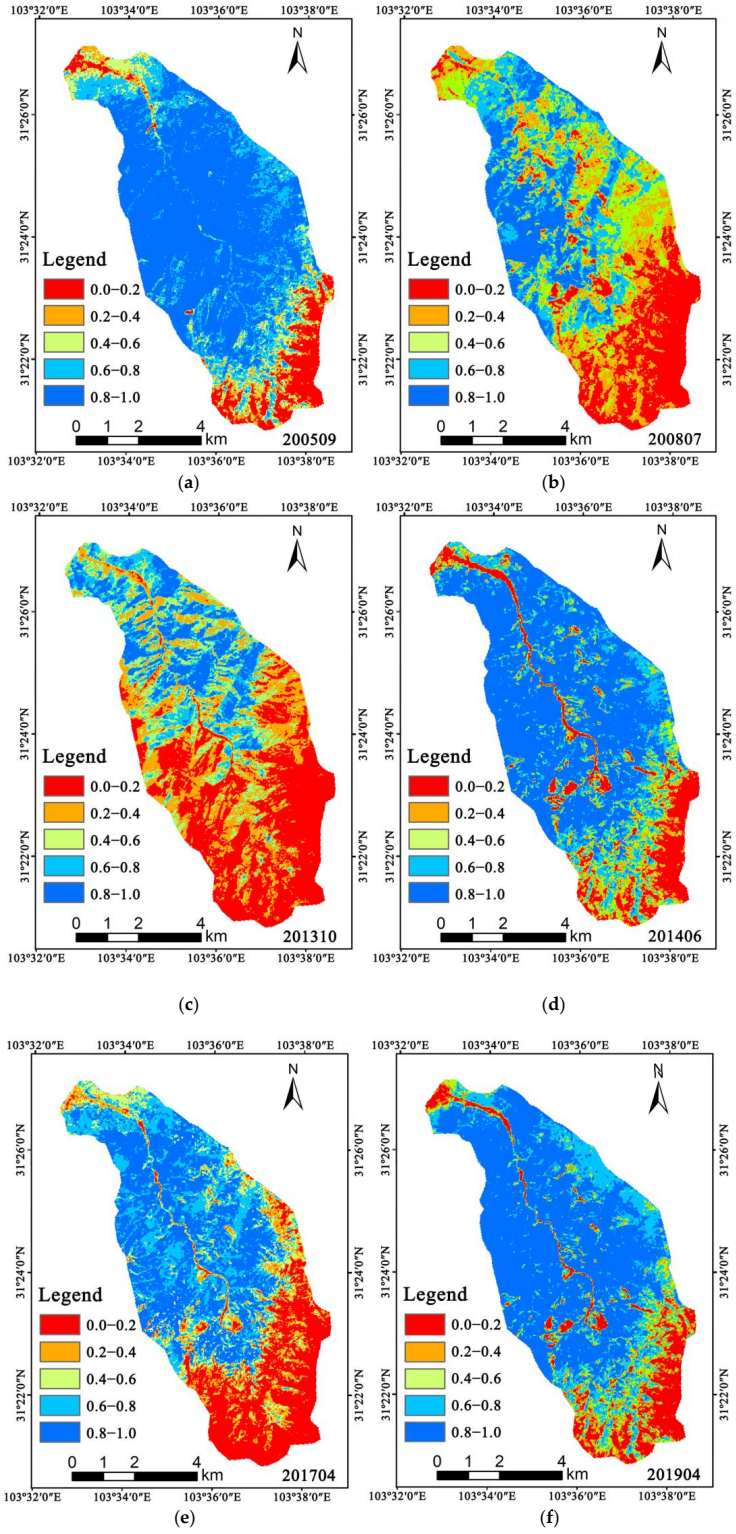

Figure 3. Variations of vegetation coverage in the Qipan gully from 2005 to 2019 (ArcGIS 10.8). (**a**) September 2005; (**b**) July 2008; (**c**) October 2013; (**d**) June 2014; (**e**) April 2017; (**f**) April 2019.

Existing studies have shown that earthquakes could cause surface disturbance and deformation, resulting in a "drag" effect that damages surface vegetation [17]. Figure 3a, b show the obvious decrease in vegetation coverage after the Wenchuan Earthquake. The comparison between Figure 3b,c indicates that the vegetation coverage reached its minimum after the large-scale debris flow that occurred on 11 July 2013. This should be attributed to the inhibition of vegetation growth caused by a large amount of gravel slope provenance and the formation of gully provenance derived from the erosion of concentrated rainfall on unstable slope provenance. According to Figure 3d,e vegetation coverage in summer is higher, which might be attributed to the influence of snow accumulation in high-altitude areas. On the whole, vegetation in the Qipan gully gradually recovered after the earthquake, and the vegetation coverage has returned to the pre-earthquake level, as shown in Figure 3f. Thus, vegetation coverage can serve as a primary indicator for the attenuation of slope activity on unstable slopes after earthquakes.

4.2. Spatiotemporal Evolution of Slope Provenance in the Qipan Gully

Due to the influence of perennial snow in high-altitude areas within the valley, it is difficult to accurately interpret the dynamic changes in debris flow slope provenance post-earthquake solely based on vegetation coverage. As a supplement and auxiliary method, this study chose high-definition Google satellite images and used the ArcGIS software (10.8) to count the slope provenance and gully provenance [38]. The high-resolution Quickbird images were imported into ArcGIS, where the area without vegetation coverage is delineated and shown in Figure 4. In Figure 4, the yellow area indicates slope provenance and the blue area is gully provenance.

According to interpretation, debris flow in this gully with existing slope provenance pre-earthquake belongs to the high-frequency torrential valley-type viscous type. By comparing Figure 4a,b it can be concluded that the amount of provenance increased significantly after the earthquake, which is consistent with the interpretation of vegetation coverage. The slight difference between the satellite image and the vegetation coverage interpretation should be attributed to the difference in resolution. Overall, as the vegetation recovers after the earthquake, the slope provenance gradually decreases. Figure 4d shows more slope provenance in 2014 than in 2011, shown in Figure 4c, which may be due to the impact of the large-scale debris flow that occurred in 2013. Figure 4e,f show that the fixation effect of vegetation on slope provenance is increasingly obvious.

4.3. Evolution of Gully Provenance by Field Investigation

To obtain detailed information on gully provenance in the Qipan gully, a field investigation and UAV exploration was carried out on 16 March 2019 (Figure 5). Due to the relatively short distance of 1# check dam and 2# pile-group dam [39–41] to the mouth of the gully, not much gully provenance could be found after dredging. As for the 3# check dam, the opening was severely blocked, resulting in its full siltation and damage to its function. The total storage capacity of the five dams in the Qipan gully is 95.6×10^4 m^3 according to a field investigation report [29] and relevant literature. Further, based on a report by Yuan et al. [39] 11 years after the earthquake, the slope provenance is not that active, and the influence of blocking structures has led to significant accumulation in the main gully. The content of the silt and clay increased significantly, accounting for 15–20%, while the content of the coarse boulders decreased to about 50%. The increase in the content of silt and clay would lead to a decrease in the hazard of debris flow, which is consistent with previous research [40].

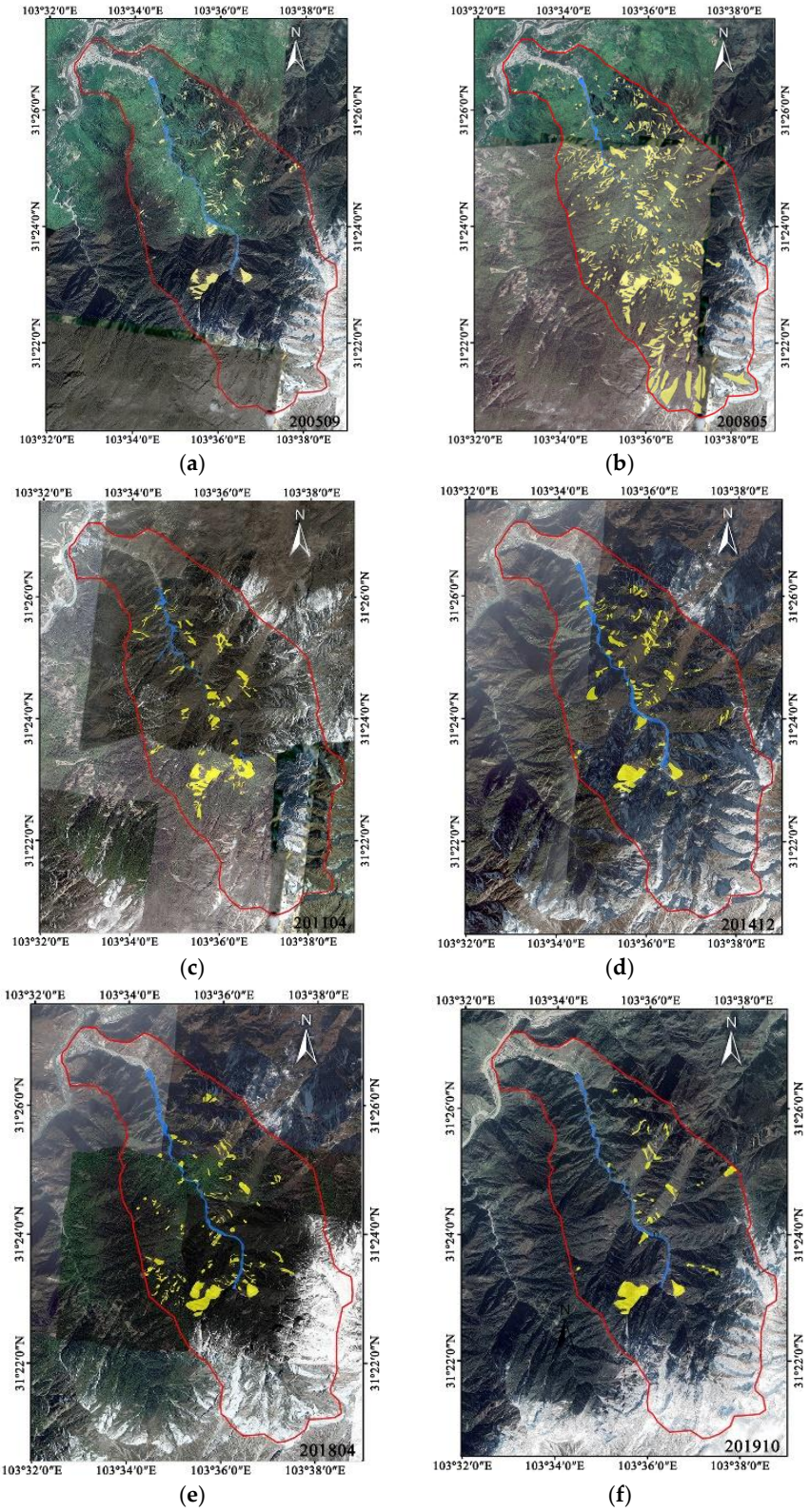

Figure 4. Materials interpretation of debris flow based on remote sensing images in the Qipan gully basin from 2005 to 2019 (ArcGIS 10.8). (**a**) September 2005; (**b**) May 2008; (**c**) April 2011; (**d**) December 2014; (**e**) April 2018; (**f**) October 2019.

Figure 5. Exploration of the Qipan gully by UAV on 18 March 2019. (**a**) filling of 3# check dam by deposits of debris flow; (**b**) slope provenance behind 2# pile-group dam; (**c**) scouring of 2# pile-group dam; (**d**) location of drinking water source; (**e**) dredging of 1# check dam; (**f**) fixation of provenance by vegetation; (**g**) 1# check dam; (**h**) gully provenance.

5. Results and Discussion

The degree of difficulty of the debris flow outbreak post-earthquake largely depends on the dynamic changes in provenance. It is necessary to multi-angle analyze the dynamic changes due to significant differences in the attenuation patterns of slope provenance and gully provenance post-earthquake and hysteresis of the changes in gully provenance. It could be seen from Figure 3 that the vegetation was severely destroyed after the Wenchuan earthquake, and most slope provenance of debris flow is mainly in the low-altitude areas (below the altitude of 2000 m). The slope provenance was distributed at an altitude of 1800–2500 m, gradually shifting to higher altitude areas with time [29]. Figure 6a shows

statistical results of the distribution of vegetation coverage. The vegetation coverage has gradually increased year by year, with a decrease in 2013 after the large-scale debris flow, and by 2019 it has reached the pre-earthquake level. Figure 4 shows the Quickbird visual interpretation results. The calculated results illustrated in Figure 6b indicate that slope provenance pre-earthquake is 7.7 times that post-earthquake. After the earthquake, slope provenance generally decreased with time, further verifying its dynamic changes.

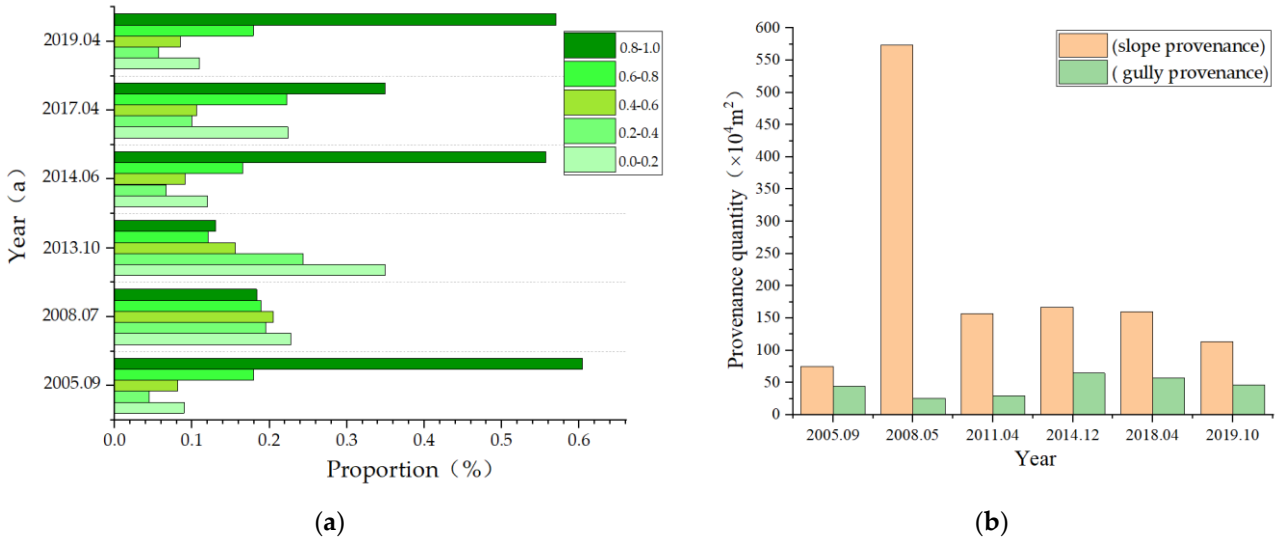

(**a**) (**b**)

Figure 6. Statistic analysis of vegetation coverage and provenance of debris flow in the Qipan gully. (**a**) Statistic analysis of vegetation coverage during 2005–2019; (**b**) Statistic analysis of slope provenance and gully provenance during 2005–2019.

To better understand the hazards of debris flow in the Qipan gully, it is necessary to assess the risk of debris flow. Firstly, a system of assessment indicators for the risk of debris flow is established, as shown in Figure 7. Based on disaster-pregnant environment and post-disaster measures, five indicators of the criterion layer, degree of difficulty B_1, meteorological condition B_2, topographic condition B_3, post-earthquake recovery B_4, and efficiency of blocking structures B_5, are employed to assess the risk of debris flow. Fourteen indicators of the indicators layer are selected in this study, including an area of slope provenance X_1 (km^2), an area of gully provenance X_2 (km^2), single outburst volume X_3 (m^3), occurrence frequency X_4 (times/ 50 years), 24 h maximum rainfall X_5 (mm), catchment area X_6 (km^2), length of main gully X_7 (km), relative elevation difference of catchment X_8 (km), catchment gully density X_9 ($km \cdot km^{-2}$), vegetation coverage X_{10} (%), the weight proportion of particles at gully mouth with a size less than 5 mm X_{11}, capacity of blocking structures X_{12}, the operating status of engineering X_{13} (%), and population density X_{14} (persons/km^2). Among them, building blocking structures would lead to a decrease in gully provenance, and, with the urbanization process, building area (human activities) increases by the year.

The risk of debris flow in a single gully post-earthquake varies dynamically, especially after the construction of block structures. According to related field investigation reports and literature [29,31], the risk assessment indicators of debris flow in the Qipan gully are graded, assigned value, and shown in Table 2. The risk is comprehensively assessed and divided into five grades: extremely low risk (I), low risk (II), moderate risk (III), high risk (IV), and extremely high risk (V), and listed in Table 3. The semi-quantitative value assignment and qualitative grading methods for indicators X_{12} and X_{13} are also shown in Figure 8.

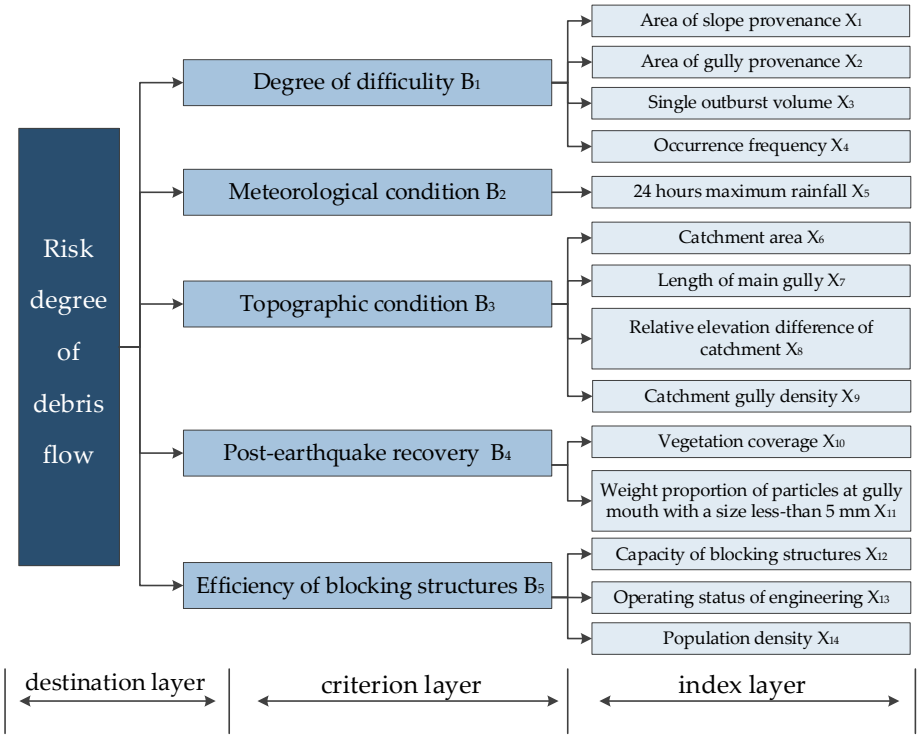

Figure 7. System of risk assessment indicators of debris flow of the Qipan gully.

Table 2. The measured value of risk assessment indicators of debris flow in the Qipan gully.

Year	X_1 (10^4 km^2)	X_2 (10^4 km^2)	X_3 (10^4 m^3)	X_4 (times/50 years)	X_5 (mm)	X_6 (km^2)	X_7 (km)	X_8 (km)	X_9 (km·km^{-2})	X_{10} (%)	X_{11} (%)	X_{12}	X_{13}	X_{14} (Population/km^2)
2005	75	34	5	20	26	54.2	15.2	3.04	2.12	60	40	0	0	90
2008	574	26	8	22	34	54.2	15.2	3.04	2.12	18	9	0	0	65
2011	157	32	8	24	38.3	54.2	15.2	3.04	2.12	24	15	0	0	135
2013	581	54	78.2	25	54.3	54.2	15.2	3.04	2.12	13	17	0	0	135
2018	149	37	11.5	27	33.4	54.2	15.2	3.04	2.12	34	30	0.6	0.8	165
2019	114	33	15	28	28.1	54.2	15.2	3.04	2.12	57	37	0.6	0.7	185

Table 3. Risk classification standard of debris flows in the Qipan gully.

Category	I	II	III	IV	V
X_1	[0~25]	[25~50]	[50~100]	[100~250]	[250~1000]
X_2	[0~10]	[10~20]	[20~30]	[30~40]	[40~60]
X_3	[0~1]	[1~5]	[5~10]	[10~100]	[100~700]
X_4	[0~5]	[5~10]	[10~20]	[20~100]	[100~150]
X_5	[0~25]	[25~50]	[50~75]	[50~100]	[100~500]
X_6	[0~0.5]	[0.5~5]	[5~15]	[15~35]	[35~70]
X_7	[0~1]	[1~2]	[2~5]	[5~10]	[10~50]
X_8	[0~0.2]	[0.2~0.5]	[0.5~0.7]	[0.7~1.0]	[1.0~6.0]
X_9	[0~2]	[2~5]	[5~10]	[10~20]	[20~100]
X_{10}	[80~100]	[80~60]	[60~40]	[20~40]	[0~20]
X_{11}	[80~100]	[80~60]	[60~40]	[20~40]	[0~20]
X_{12} [41] *	[0.8~1]	[0.6~0.8]	[0.4~0.6]	[0.2~0.4]	[0~0.2]
X_{13} [42] *	[0.8~1]	[0.6~0.8]	[0.4~0.6]	[0.2~0.4]	[0~0.2]
X_{14}	[0~20]	[20~50]	[50~100]	[100~200]	[200~3000]

* X_{12}: newly built (I); 1/3 storage capacity silted (II); 2/3 storage capacity silted (III); fully silted (IV); not built (V).
* X_{13}: foundation, abutment, body, and overflow port of dam not damaged and weep hole not clogged (I); dam foundation not scoured, a small part of abutment, body, and overflow port of dam damaged and weep hole not clogged (II); dam foundation not scoured, a small part of abutment, body, and overflow port of dam damaged and weep hole less clogged (III); dam foundation scoured, abutment, body, and overflow port of dam damaged and weep hole less clogged (IV); dam foundation seriously scoured, abutment, body, and overflow port of dam seriously damaged and weep hole completely clogged (V).

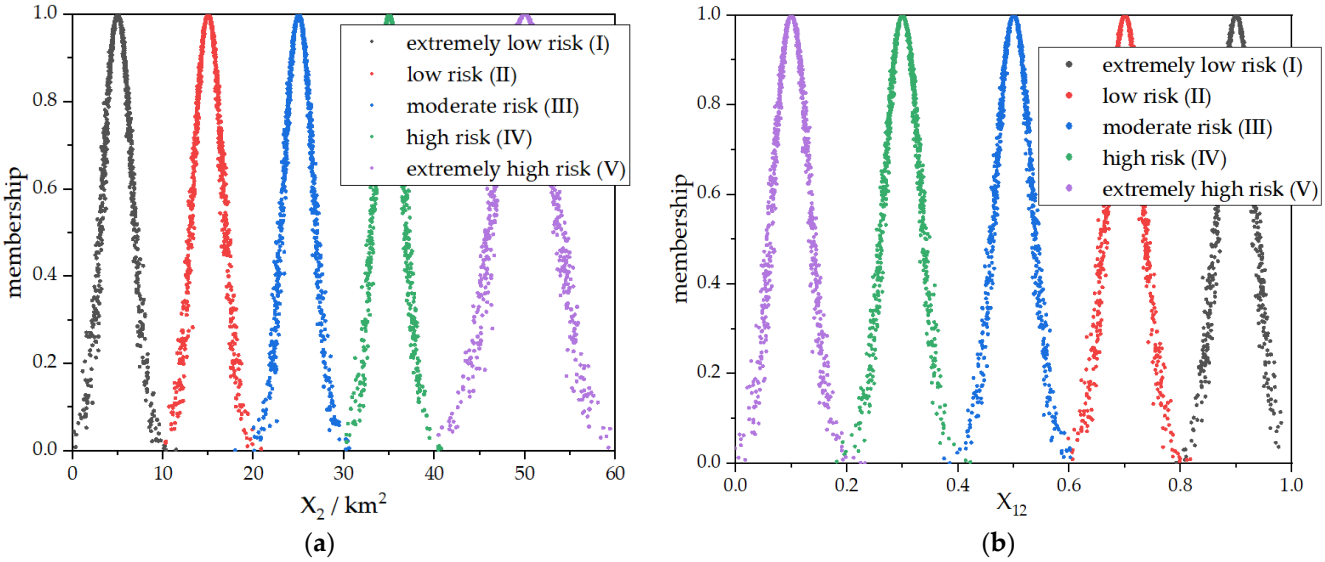

Figure 8. Cloud model of assessment grade of area of gully provenance X_2 (**a**) and capacity of blocking structures X_{12} (**b**).

In consideration of the 14 assessment indicators, a cloud model corresponding to five risk levels is established based on Equations (19)–(23). According to the game theory combination weighting method, the optimal combination weight w* is obtained as (0.09, 0.20, 0.06, 0.02, 0.11, 0, 0, 0, 0, 0.07, 0.03, 0.18, 0.19, and 0.05) and imported into the cloud model. The calculated results of the characteristic parameters of each assessment indicator of debris flow in the Qipan gully are listed in Table 4. Based on Equation (23), a cloud map for each assessment indicator could be generated by MATLAB. During this process, a risk assessment of debris flow in the Qipan gully is conducted on a time scale. For better expression, the indicators X_2 and X_{12} highly correlated with the dynamic changes in provenance, and are selected to generate cloud maps, shown in Figure 8.

Table 4. Risk assessment results of debris flow in the Qipan gully during 2005–2019.

Year	Risk Assessment Value					Risk Grade
	I	II	III	IV	V	
2005	0.0009	0.0046	0.2282	0.1015	0.0237	moderate risk
2008	0.0002	0.0126	0.0489	0.0011	0.1572	extremely high risk
2011	0.0019	0.0019	0.0752	0.1430	0.0936	high risk
2013	0.0001	0.0002	0.0245	0.1327	0.1657	extremely high risk
2018	0.0235	0.1280	0.0000	0.2366	0.0006	high risk
2019	0.0007	0.3534	0.0084	0.1210	0.0005	low risk

Table 4 lists the risk assessment results of debris flow in the Qipan gully during 2005–2019. In 2005 before the Wenchuan earthquake, the risk level was "moderate", which confirms that this gully is an old debris flow gully. In 2008, the early stage after the earthquake, the risk level had become extremely high. The main reasons for this were the surface disturbance, vegetation damage, and variations in hydrological conditions caused by the earthquake, which made a 15–20% decrease in early rainfall and a 25–30% decrease in hourly rainfall intensity that triggered the debris flow post-earthquake [43]. By 2011, there had been no record of debris flow disasters, which should be attributed to the decrease in gully provenance induced by the reconstruction post-earthquake and no extreme rainfall. Although there was a relatively short supply of slope provenance, there

is still plenty of slope provenance present, and the risk level is high. After the large-scale debris flow in 2013, the risk level became extremely high. This is primarily due to long periods of heavy rainfall causing an infiltration of rainwater into slopes at both sides of the gully, resulting in an increased pore water pressure and unit weight and a decreased shear resistance and stability. Thus, loose particles and debris along both sides of the gully (lateral erosion) and in the gully (bottom erosion) were involved in the debris flow. As the provenance decreases, the risk of debris flow gradually decreases. In 2018 and 2019, the risk levels of debris flow were reduced to high risk and low risk, respectively. This was mainly due to the increase in vegetation, which reduced soil erosion and improved the stability of slopes. In addition, the interception of rainfall by tree canopies and leaf litter, as well as the prevention of rainwater infiltration, could reduce surface runoff and prevent surface soil erosion. Meanwhile, the roots of plants could further strengthen the slope soil, thereby reducing the risk of debris flow.

6. Conclusions

Two field investigations carried out in 2019 and 2021 in the Qipan gully in Wenchuan County found that the vegetation coverage of the mountain about 10 years after the earthquake is consistent with that of pre-earthquake. In comparison with pre-earthquake, abundant provenance in the gully closely related to debris flow post-earthquake, with an increased risk of debris flow under the effect of rainfall. This study adopts multiple methods to explore the dynamic variation in debris flow and analyze the risk of debris flow dynamically [12,43]. The main conclusions were drawn as follows:

- In the early stage post-earthquake (2008–2013), the main material source of debris flow was slope provenance, and after 2018 it shifted to gully provenance. The absence of debris flow hazards from 2014 to 2018 was mainly due to the construction of block structures. In the assessment of the risk of debris flow, it is more realistic to take the blocking structures into account alongside significant factors such as dynamic variations in provenance and precipitation.
- Five blocking dams with a total storage capacity of 95.6×10^4 m^3 were constructed in 2014 and the estimated annual dredging volume is 50.3×10^4 m^3. Based on the field investigation and references, it is estimated that by 2019, within 11 years after the Wenchuan earthquake and through many outbreaks of debris flow and continuous dredging, about 781.3×10^4 m^3 of the provenance of debris flow was discharged out of the gully mouth.
- Quickbird visual interpretation results indicate that the slope provenance pre-earthquake is 7.7 times that post-earthquake. Multi-type remote sensing information reveals that vegetation had recovered to the pre-earthquake level by 2019.
- It is more realistic to employ game theory combined with the cloud model to assess the hazard of debris flow in the Qipan gully, and this method could be used to dynamically assess hazards of the debris flow of a single gully.

More than 10 years have passed since the Wenchuan earthquake. The comparison shows that the hourly rainfall intensity triggering the debris flow in the Qipan gully in 2019 is 24 mm, about 2/3–4/5 of the pre-earthquake level, which is consistent with previous research. An obvious characteristic of the debris flow post-earthquake is that the risk generally decreases with the decrease in provenance, which is verified by plenty of previous research. It is found that with the gradual covering of the slope by provenance originating from an earthquake by vegetation recovery, gully provenance becomes the dominant factor in the outburst of debris flow. The field investigations reveal that the dynamic variation in gully provenance is controlled by both natural and human factors. To be more specific, gully provenance is continuously supplied by slope provenance and reduced by outbursts of debris flow and the dredging of blocking structures. Multi-type and multi-scale monitoring methods are employed to ascertain the provenance of debris flow and a risk assessment model based on game theory and the cloud model is constructed to dynamically assess the risk of debris flow in the Qipan gully from 2005 to 2019. There are

also limitations in the research, such as that it has been conducted over a long period of time, that there has been a continuous development of remote sensing technology, the existence of glacier erosion landforms, and the long distance between the rainfall station at the gully mouth and provenance areas, which would lead to errors in the assessment. On the whole, the multi-type and multi-scale monitoring method and field investigation in this study is feasible in the dynamic assessment of the risk of debris flow in the Qipan gully. It should be noted that in future research advanced technologies such as weather radar and satellite data assimilation should be adopted to obtain more accurate and timely rainfall patterns and intensity information, and real-time data obtained from advanced technologies should be combined with a risk assessment model based on game theory and the cloud model to enhance prediction and assessment of the risk of debris flow. The dynamic assessment of the risk of debris flow with the process of "assessment-feedback-adjustment-reassessment" would be helpful in the increase in prediction precision of the risk of future debris flow, and the implementation of "prevent disasters before happen and reduce loss after happen". In general, future research on debris flow should be devoted to deepening the understanding of potential disaster factors of debris flow and developing more accurate prediction and evaluation models. This would help in developing effective disaster reduction strategies, protecting the life and infrastructure in debris flow-prone areas, and providing reference and guidance for future construction in earthquake-prone mountain areas.

Author Contributions: Conceptualization, N.S.; writing—original draft, B.Y. and F.G.; data curation, N.S., Y.L. and L.X.; visualization, N.S. and F.G.; supervision, N.S. and Y.L.; funding acquisition, L.X. All authors have read and agreed to the published version of the manuscript.

Funding: This research was funded by the National Natural Science Foundation of China (No. U2268213), the National Key Research and Development Program of China (Grant No. 2018YFC1505403), and the National Natural Science Foundation of China (Grant No. 42172322). This research was funded by the Henan Key Scientific and Technological Project (Grant No. 212102110200) and the Open Research Subject of Henan Key Laboratory of Grain and Oil Storage Facility & Safety (Grant No. 2022KF06).

Institutional Review Board Statement: Not applicable.

Informed Consent Statement: Not applicable.

Data Availability Statement: Data sharing is not applicable to this article.

Acknowledgments: We thank Sichuan Huadi Construction Engineering Co., Ltd. for supplying the field investigation report. We would like to thank the anonymous reviewers for their valuable comments.

Conflicts of Interest: The authors declare no conflict of interest.

References

1. Dai, F.C.; Xu, C.; Yao, X.; Xu, L.; Tu, X.B.; Gong, Q.M. Spatial distribution of landslides triggered by the 2008 Ms. 8.0 Wenchuan earthquake, China. *J. Asian Earth Sci.* **2011**, *40*, 883–895. [CrossRef]
2. Chang, M.; Tang, C.; Van Asch, T.W.; Cai, F. Hazard assessment of debris flows in the Wenchuan earthquake-stricken area South West China. *Landslides* **2017**, *14*, 1783–1792. [CrossRef]
3. Fan, X.M.; Scaringi, G.; Domènech, G.; Yang, F.; Guo, X.J.; Dai, L.X.; He, C.Y.; Xu, Q.; Huang, R.Q. Two multi-temporal datasets that track the enhanced landsliding after the 2008 Wenchuan earthquake. *Earth Syst. Sci. Data* **2019**, *11*, 35–55. [CrossRef]
4. Li, N.; Tang, C.; Zhang, X.Z.; Chang, M.; Shu, Z.L.; Bu, X.H. Characteristics of the disastrous debris flow of chediguan gully in yinxing town, Sichuan province, on August 20, 2019. *Sci. Rep.* **2021**, *11*, 23666. [CrossRef]
5. Huang, R.Q. Geo-engineering lessons learned from the 2008 Wenchuan earthquake in Sichuan and their significance to reconstruction. *J. Mt. Sci.* **2011**, *8*, 176–189. [CrossRef]
6. Yang, W.T.; Qi, W.W.; Zhou, J.X. Decreased post-seismic landslides linked to vegetation recovery after the 2008 Wenchuan earthquake. *Ecol. Indic.* **2018**, *89*, 438–444. [CrossRef]
7. Fan, R.L.; Zhang, L.M.; Wang, H.J.; Fan, X.M. Evolution of debris flow activities in Gaojiagou Ravine during 2008–2016 after the Wenchuan earthquake. *Eng. Geol.* **2018**, *235*, 1–10. [CrossRef]
8. Chen, M.; Tang, C.; Xiong, J.; Shi, Q.Y.; Li, N.; Gong, L.F.; Wang, X.D.; Tie, Y. The long-term evolution of landslide activity near the epicentral area of the 2008 Wenchuan earthquake in China. *Geomorphology* **2020**, *367*, 107317. [CrossRef]
9. Yang, F.; Fan, X.; Siva Subramanian, S.; Dou, X.; Xiong, J.; Xia, B.; Yu, Z.; Xu, Q. Catastrophic debris flows triggered by the 20 August 2019 rainfall, a decade since the Wenchuan earthquake, China. *Landslides* **2021**, *18*, 3197–3212. [CrossRef]

10. Fan, X.; Domènech, G.; Scaringi, G.; Huang, R.; Xu, Q.; Hales, T.C.; Dai, L.; Yang, Q.; Francis, O. Spatio-temporal evolution of mass wasting after the 2008 Mw 7.9 Wenchuan earthquake revealed by a detailed multi-temporal inventory. *Landslides* **2018**, *15*, 2325–2341. [CrossRef]
11. Liu, J.F.; You, Y.; Chen, X.Q.; Chen, X.Z. Mitigation planning based on the prediction of river blocking by a typical large-scale debris flow in the Wenchuan earthquake area. *Landslides* **2016**, *13*, 1231–1242. [CrossRef]
12. Wang, L.; Chang, M.; Le, J.; Xiang, L.L.; Ni, Z. Two multi-temporal datasets to track debris flow after the 2008 Wenchuan earthquake. *Sci. Data* **2022**, *9*, 525. [CrossRef]
13. Tang, C.X.; Liu, X.L.; Cai, Y.H.; Van Westen, C.; Yang, Y.; Tang, H.; Yang, C.Z.; Tang, C. Monitoring of the reconstruction process in a high mountainous area affected by a major earthquake and subsequent hazards. *Nat. Hazards Earth Syst. Sci.* **2020**, *20*, 1163–1186. [CrossRef]
14. Yuan, B.X.; Chen, W.J.; Zhao, J.; Li, L.J.; Liu, F.; Guo, Y.C.; Zhang, B.F. Addition of alkaline solutions and fibers for the reinforcement of kaolinite-containing granite residual soil. *Appl. Clay Sci.* **2022**, *228*, 106644. [CrossRef]
15. Chen, M.; Tang, C.; Zhang, X.Z.; Xiong, J.; Chang, M.; Shi, Q.Y.; Wang, F.L.; Li, M.W. Quantitative assessment of physical fragility of buildings to the debris flow on 20 August 2019 in the Cutou gully, Wenchuan, southwestern China. *Eng. Geol.* **2021**, *293*, 106319. [CrossRef]
16. Cui, P.; Xiang, L.Z.; Zou, Q. Risk assessment of highways affected by debris flows in Wenchuan earthquake area. *J. Mt. Sci.* **2013**, *10*, 173–189. [CrossRef]
17. Li, Y.W.; Xu, L.R.; Gu, F.Y.; Su, N.; Zhang, L.L. Influence of disaster-pregnant factors on debris flow hazard. *Earth Sci.* **2022**, 1–12. (In Chinese)
18. Ouyang, C.J.; Wang, Z.W.; An, H.C.; Liu, X.R.; Wang, D.P. An example of a hazard and risk assessment for debris flows—A case study of Niwan Gully, Wudu, China. *Eng. Geol.* **2019**, *263*, 105351. [CrossRef]
19. Yan, J.T.; Liu, S.G. Cloud model evaluation of autonomous capability of ground-attack UAV based on combined weighting. *J. Beijing Univ. Aeronaut. Astronaut* **2022**, 1–14.
20. Wang, M.W.; Wang, Y.; Shen, F.Q.; Jin, J.L. Projection pursuit method based on connection cloud model for assessment of debris flow disasters. *J. Environ. Inform.* **2023**, *41*, 118–129. [CrossRef]
21. Yuan, B.X.; Chen, W.J.; Li, Z.H.; Zhao, J.; Luo, Q.Z.; Chen, W.W.; Chen, T.Y. Sustainability of the polymer SH reinforced recycled Granite Residual Soil: Properties, physicochemical mechanism and applications. *J. Soils Sediments* **2023**, *23*, 246–262. [CrossRef]
22. Yin, L.Z.; Zhu, J.; Li, Y.; Zeng, C.; Zhu, Q.; Qi, H.; Liu, M.W.; Li, W.L.; Cao, Z.Y.; Yang, W.J.; et al. A virtual geographic environment for debris flow risk analysis in residential areas. *ISPRS Int. J. Geo. Inf.* **2017**, *6*, 377. [CrossRef]
23. Xu, X.Y.; Wang, M.W.; Li, Y.F.; Zhang, L.B. Risk evaluation of debris flow hazard based on asymmetric connection cloud model. *Math. Probl. Eng.* **2017**, *2017*, 5348149. [CrossRef]
24. Zhu, J.; Tang, C.; Chang, M.; Le, M.H.; Huang, X. Field Observations of the Disastrous 11 July 2013 Debris Flows in Qipan Gully, Wenchuan Area, Southwestern China. In *Engineering Geology for Society and Territory—Volume 2*; Springer: Berlin/Heidelberg, Germany, 2015; pp. 531–535.
25. Hu, T.; Huang, R.Q. A catastrophic debris flow in the Wenchuan Earthquake area, July 2013: Characteristics, formation, and risk reduction. *J. Mt. Sci.* **2017**, *14*, 15–30. [CrossRef]
26. Ding, M.T.; Huang, T. Vulnerability assessment of population in mountain settlements exposed to debris flow: A case study on Qipan gully, Wenchuan County, China. *Nat. Hazards* **2019**, *99*, 553–569. [CrossRef]
27. Hu, X.D.; Yang, F.; Hu, K.H.; Ding, M.; Liu, S.; Wei, L. Estimating the debris-flow magnitude using landslide sediment connectivity, Qipan catchment, Wenchuan County, China. *Catena* **2023**, *220*, 106689. [CrossRef]
28. Shi, Q.Y.; Tang, C.; Gong, L.F.; Chen, M.; Li, N.; Zhou, W.; Xiong, J.; Tang, H.; Wang, X.D.; Li, M.W. Activity evolution of landslides and debris flows after the Wenchuan earthquake in the Qipan catchment, Southwest China. *J. Mt. Sci.* **2021**, *18*, 932–951. [CrossRef]
29. *Investigation of Emergency Actions to Mitigate Debris Flow Hazards in the Qipan Gully, Wenchuan County, Aba Prefecture, Sichuan Province*; Sichuan Shutong Geotechnical Engineering Co., Ltd.: Ya'an, China, 2013.
30. *Field Investigation Report on Emergency Management Project of Landslide and Debris Flow in the Qipan Gully in Wenchuan County, Aba Prefecture, Sichuan Province*; Sichuan Huadi Construction Engineering Co., Ltd.: Chengdu, China, 2008.
31. Yunus, A.P.; Fan, X.M.; Tang, X.L.; Jie, D.; Xu, Q.; Huang, R.Q. Decadal vegetation succession from MODIS reveals the spatio-temporal evolution of post-seismic landsliding after the 2008 Wenchuan earthquake. *Remote Sens. Environ.* **2020**, *236*, 111476. [CrossRef]
32. Chen, M.; Tang, C.; Li, M.W.; Xiong, J.; Luo, Y.T.; Shi, Q.Y.; Zhang, X.Z.; Tie, Y.; Feng, Q. Changes of surface recovery at coseismic landslides and their driving factors in the Wenchuan earthquake-affected area. *Catena* **2022**, *210*, 105871. [CrossRef]
33. Chen, C.-C.; Tseng, C.-Y.; Dong, J.-J. New entropy-based method for variables selection and its application to the debris-flow hazard assessment. *Eng. Geol.* **2007**, *94*, 19–26. [CrossRef]
34. Li, J.Q.; Fan, T.C.; Zhou, Y.R.; Fang, Q. Comprehensive evaluation on capability of civil aviation supervisor team based on cloud model. *J. Beijing Univ. Aeron. Astron* **2022**, *48*, 2425–2433. (In Chinese)
35. Tang, J.W.; Wang, D.; Ye, W.; Dong, B.; Yang, H.J. Safety Risk Assessment of Air Traffic Control System Based on the Game Theory and the Cloud Matter Element Analysis. *Sustainability* **2022**, *14*, 6258. [CrossRef]

36. Zou, Q.; Liao, L.; Qin, H. Fast Comprehensive Flood Risk Assessment Based on Game Theory and Cloud Model Under Parallel Computation (P-GT-CM). *Water Resour. Manag.* **2020**, *34*, 1625–1648. [CrossRef]
37. Cao, C.; Xu, P.H.; Chen, J.P.; Zheng, L.J.; Niu, C.C. Hazard assessment of debris-flow along the baicha river in Heshigten Banner, Inner Mongolia, China. *Int. J. Environ. Res. Public Health* **2017**, *14*, 30. [CrossRef]
38. Zhang, X.Z.; Tang, C.X.; Li, N.; Xiong, J.; Chen, M.; Li, M.W.; Tang, C. Investigation of the 2019 Wenchuan County debris flow disaster suggests nonuniform spatial and temporal post-seismic debris flow evolution patterns. *Landslides* **2022**, *19*, 1935–1956. [CrossRef]
39. Yuan, Y.D. *Starting Mechanism of "Wide and Gentle" Channel Source in Strong Earthquake Zone and Research on Evaluation of Dynamic Reserves: Taking QiPan Ditch as an Example*; Southwest University of Science and Technology: Mianyang, China, 2020.
40. Egbueri, J.C.; Igwe, O. Development of a novel numerical indicator (DLPI) for assessing the detachability and liquefaction potentials of soils in erosion-prone areas. *Model Earth Syst. Environ.* **2021**, *7*, 2407–2429. [CrossRef]
41. Zhang, W.T.; Liu, J.F.; You, Y.; Sun, H.; Yang, H.Q.; Lu, M. Damage evaluation of control works against debris flow: A case study in Wenchuan area. *J. Geol. Hazard Control* **2022**, *33*, 77–83. (In Chinese)
42. Zhang, W.T.; Liu, J.F.; You, Y.; Sun, H.; Yang, H.Q.; Lu, M. Analysis and Evaluation of the Treatment Effect of the Geotechnical Engineering of Debris Flow: Case of Xingfu Gully in Wolong. *J. Catastrophology* **2021**, *36*, 208–214. (In Chinese)
43. Fan, X.M.; Juang, C.H.; Wasowski, J.; Huang, R.Q.; Xu, Q.; Scaringi, G.; van Westend, C.J.; Havenith, H.B. What we have learned from the 2008 Wenchuan Earthquake and its aftermath: A decade of research and challenges. *Eng. Geol.* **2018**, *241*, 25–32. [CrossRef]

Disclaimer/Publisher's Note: The statements, opinions and data contained in all publications are solely those of the individual author(s) and contributor(s) and not of MDPI and/or the editor(s). MDPI and/or the editor(s) disclaim responsibility for any injury to people or property resulting from any ideas, methods, instructions or products referred to in the content.